Mathematical Biosciences and Engineering

http://www.aimspress.com/journal/mbe

MBE, 20(7): 13334–13355.
DOI: 10.3934/mbe.2023594
Received: 20 April 2023
Revised: 08 May 2023
Accepted: 15 May 2023
Published: 09 June 2023

Research article

Direct yaw-moment control of electric vehicles based on adaptive sliding mode

Li Ma[1,*], Chang Cheng[1], Jianfeng Guo[1], Binhua Shi[2], Shihong Ding[1] and Keqi Mei[1,2]

[1] School of Electrical and Information Engineering, Jiangsu University, Zhenjiang 212013, China
[2] Zhejiang JIALIFT Warehouse Equipment Co., Ltd., Huzhou 313104, China

* **Correspondence:** Email: mali@ujs.edu.cn.

Abstract: The direct yaw-moment control (DYC) system consisting of an upper controller and a lower controller is developed on the basis of sliding mode theory and adaptive control technique. First, the two-degree of freedom (2-DOF) model is utilized to calculate the ideal yaw rate. Then, the seven-degree of freedom (7-DOF) electric vehicle model is given to design the upper controller by employing first-order sliding mode (FOSM) method, which is constructed to guarantee the actual yaw rate to approach the ideal value and gain the additional yaw moment. On this basis, an adaptive first-order sliding mode (AFOSM) controller is designed to enhance the system robustness against probable modelling error and parametric uncertainties. In order to mitigate the chattering issue present in the FOSM controller, a novel adaptive super-twisting sliding mode (ASTSM) controller is proposed for the design of DYC. Furthermore, the lower controller converting the additional yaw moment into driving or braking torque acting on each wheel is also developed. Finally, The simulation results indicate that the proposed DYC system can improve the electric vehicle driving stability effectively.

Keywords: sliding mode control; direct yaw-moment control; finite-time convergence

1. Introduction

With the development of industry, automobile plays an irreplaceable role in daily life. However, many environmental problems have arisen from the extensive use of vehicles. Although electric vehicles can temporarily relax the problem of air pollution, people have been concerned about its security when driving at high speed or low adhesion roads [1–4]. Recently, vehicle stability control has become a research hotspot to reduce traffic accidents. As compared to active front steering (AFS) [5–7] and antilock braking system (ABS) [8], DYC is performed by the difference between motor torques in the left and the right side of the vehicle. Since each wheel can be controlled individually by the in-wheel-motor-drive electric vehicle (IWM-EV), the DYC can be implemented

on IWM-EV appropriately [9]. Overall, the DYC system helps improve the vehicle stability, handling and safety, particularly in the situations where the driver may need to make sudden evasive maneuvers or encounter adverse weather or road conditions [10–13].

There are numerous nonlinear control methods [14–19] for DYC. For example, in [10], the introduced nonsmooth state feedback approach provides the better control accuracy via the finite-time control, the second-order sliding mode (SOSM) observer and nonlinear disturbance observer (NDOB) techniques. In [20], the fuzzy logic [21] was used in DYC to improve the vehicle stability. In [22], a robust H_∞ control [23] method based on vehicle system dynamics is proposed by using linear matrix inequality. In [24], the DYC is composed of two coordinated Lyapunov model-based controllers to track the stability index, which avoids the conflict between maneuverability and stability. In addition to the above control methods, the sliding mode control (SMC) [25–27] is extensively applied in DYC as well, which is independent on mathematical models of controlled objects and possesses strong robustness against disturbances and uncertainties. In [28], a composite controller is developed to decrease the influence of external disturbances by utilizing SOSM theory and NDOB technique. Compared with traditional sliding mode controllers, the SOSM controller maintains the vehicle's stability and reduces the chattering [29]. It is well-known that the adaptive control technique is a class of control methods used in engineering and control theory that enables a system to adjust and adapt to the changes in its environment or operating conditions. The basic idea behind the adaptive control is to use the feedback from the system to update its control parameters in real time [30]. As described in [30], with the aim of improving the control performance of vehicle, an AFOSM control method was proposed to fit the change of sideslip angle and enhance the vehicle's robustness against parametric variations and uncertainties by utilizing a variable sliding mode gain. In [31], a Cybertwin driven multimodal network structure for electrocardiogram patterns monitoring was presented by using the deep learning model. In [32], a Center-based Transfer Feature Learning with Classifier Adaptation for surface defect recognition was given. It can be found from [33] that the adaptive SMC (ASMC) scheme was presented to address the issue of overestimation and underestimation in switching gains without making any assumptions beforehand about the upper bounds of the system uncertainties. In fact, the chattering always exists in the FOSM controller owing to discontinuous sign functions [34–38]. In the control of vehicle system, the chattering can be reduced by using the saturation functions instead of the discontinuous sign functions, while the robustness will be significantly weakened and the control accuracy will be reduced meanwhile [39]. Furthermore, most control algorithms used to handle the vehicle stability usually assume that the key parameters of the vehicle dynamics are known. Nevertheless, these parameters, such as the distances between the center of mass and the front or rear axles, are usually difficult to measure in several actual extreme conditions.

To fix the above problems, this paper develops two kinds of improved sliding mode controllers based on the FOSM. On the one hand, an AFOSM controller with parameter adaptation laws is designed. The adaptive laws are utilized to estimate unknown parameters in electric vehicle models, and thus the gain of the FOSM algorithm can be reduced, which avoids heavy chatting problems. On the other hand, the idea of the super-twisting algorithm (STA) has been utilized to put the discontinuous terms into the derivative of the sliding variable. Consequently, the actual control input can be obtained by integrating the discontinuous control, which will fundamentally reduce the chattering. By comparison with the existing works, the novelty and significance of this paper can be summarized as the two points. First,

different from the controllers given in [10, 20, 22], an ASTSM controller is developed by combining adaptive control technique and STA to avoid the issue of excessive fixed gain estimation, which further weakens the chattering. Second, unlike the existing adaptive laws, the adaptive law does not need to adopt the form of piecewise function, which reduces the complexity of the parameter adjustment process.

2. Electric vehicle dynamic model and control strategy structure

We will present the 2-DOF electric vehicle dynamic model first, which will be used to calculate the desired value of yaw rate. Then, the comprehensive 7-DOF model will be given to design the upper controller.

2.1. 2-DOF electric vehicle dynamic model

The 2-DOF electric vehicle model is widely used for analyzing vehicle yaw stability control. The motion equation of the electric vehicle is given by [40]

$$\dot{\beta} = \frac{k_1 + k_2}{mu}\beta + \left(\frac{ak_1 - bk_2}{mu^2} - 1\right)\omega_r - \frac{k_1}{mu}\delta_f \tag{2.1}$$

$$\dot{\omega}_r = \frac{ak_1 - bk_2}{I_z}\beta + \frac{a^2k_1 + b^2k_2}{I_z u}\omega_r - \frac{ak_1}{I_z}\delta_f \tag{2.2}$$

where m indicates the electric vehicle total mass, u is the longitudinal speed at the center of gravity of electric vehicle, k_1 and k_2 are the front-wheel and rear-wheel corning stiffness, a and b respectively represent the distances from the front and rear axles to the electric vehicle center of gravity, I_z is the total yaw moment of inertia about the z-axis, β is the ratio of longitudinal speed to lateral speed to express the sideslip angle, ω_r indicates the yaw rate, δ_f is the steering angle of the front wheels.

Remark 1: The 2DOF model cannot be used in the DYC algorithm. It is because the realization of DYC algorithm is based on yaw-moment M_z which is generated by the torque difference between right and left wheels. However, the 2DOF model regards the right and left wheels as one wheel so that the 2DOF model does not include M_z.

2.2. 7DOF electric vehicle dynamic model

The 7DOF model is introduced as follows [41], which contains the lateral, longitudinal and yaw motions of the electric vehicle body, as well as the rotational dynamics of four wheels, as shown by Figure 1.

(1) The longitudinal motion is given as

$$m(\dot{V}_x - \dot{V}_y\omega_r) = (F_{xfl} + F_{xfr})\cos\delta - (F_{yfl} + F_{yfr})\sin\delta + F_{xrl} + F_{xrr}. \tag{2.3}$$

(2) The lateral motion is established as

$$m(\dot{V}_y + V_x\omega_r) = (F_{yfl} + F_{yfr})\cos\delta + (F_{xfl} + F_{xfr})\sin\delta + F_{yrl} + F_{yrr}. \tag{2.4}$$

(3) The yaw motion is expressed as

$$I_z\dot{w}_r = a\left(F_{yfl} + F_{yfr}\right)\cos\delta + \frac{d_f}{2}\left(F_{yfl} - F_{yfr}\right)\sin\delta - b\left(F_{yrl} + F_{yrr}\right) + M_z \tag{2.5}$$

with $M_z = \frac{d_f}{2}(F_{xfr} - F_{xfl})\cos\delta + a(F_{xfl} + F_{xfr})\sin\delta + \frac{d_r}{2}(F_{xrr} - F_{xrl})$.

(4) The wheel rotational dynamics can be shown by

$$J_w\dot{\omega}_{ij} = T_{dij} - T_{bij} - F_{xij}R_{ij} \tag{2.6}$$

where i is rear (r) or front (f) wheel, j is right (r) or left (l) wheel; J_ω is the moment of inertia of the wheel, F_{xij} and F_{yij} denotes the tire's longitudinal force and lateral force, d_i is track width, T_{bij} is the braking torque, T_{dij} is the driving torque, ω_{ij} is the wheel angular velocity and R_{ij} is the rolling radius of the tire.

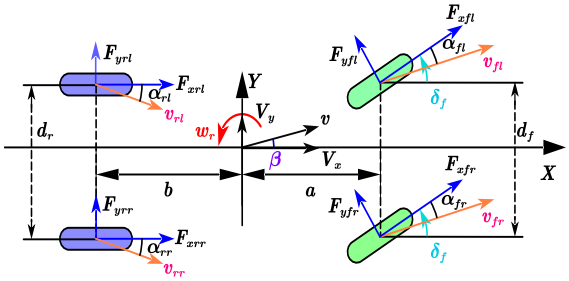

Figure 1. 7-DOF electric vehicle model.

2.3. *Problem formulation*

To keep the electric vehicle drive safely, reference values of the yaw rate and sideslip angle are calculated by 2DOF models (2.1) and (2.2) as follows

$$\omega_{rd} = min\left\{\left|\frac{u}{L(1+Ku^2)}\delta_f\right|, \left|\frac{\mu g}{u}\right|\right\} sign\left(\delta_f\right) \tag{2.7}$$

$$\beta_d = 0, \tag{2.8}$$

where μ is the road adhesion coefficient and K is the steering coefficient.

The block diagram of control structure is described in Figure 2. One can observe that the upper controller, which provides additional yaw moment, is constructed to make the actual yaw rate and the sideslip angle approach the target value. Since the sideslip angle changes greatly in case of collision and other accidents, the performance of the electric vehicle will be improved by controlling the yaw rate. Then, the lower controller distributes the torque from the upper controller to four wheels.

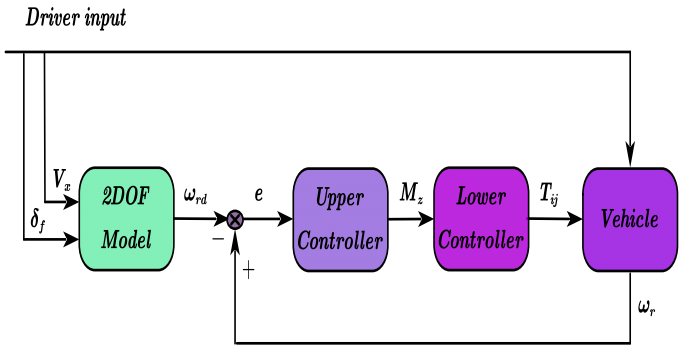

Figure 2. The diagram of DYC structure.

3. Controller design

3.1. Upper controller

First of all, we construct the DYC controller by using the traditional SMC and adaptive control technique. On this basis, we will apply the STA for the chattering reduction.

3.1.1. FOSM controller design

For the real yaw rate and its desired value, the sliding surface can be designed as

$$s = \omega_r - \omega_{rd}. \tag{3.1}$$

Taking the derivative of (3.1) produces

$$\dot{s} = \dot{\omega}_r - \dot{\omega}_{rd}. \tag{3.2}$$

Substituting (2.5) into (3.2) gets

$$\dot{s} = \frac{1}{I_z}[a\left(F_{yfl} + F_{yfr}\right)\cos\delta + \frac{d_f}{2}\left(F_{yfl} - F_{yfr}\right)\sin\delta - b\left(F_{yrl} + F_{yrr}\right) + M_z - I_z\dot{\omega}_{rd}]. \tag{3.3}$$

Denote the following term as the lumped disturbance

$$\begin{aligned} d_1(t) = \frac{1}{I_z}[&(a-\hat{a})(F_{yfl} + F_{yfr})\cos\delta + (\frac{d_f}{2} - \frac{\hat{d}_f}{2})(F_{yfl} - F_{yfr})\sin\delta \\ &- (b-\hat{b})(F_{yrl} + F_{yrr})] \end{aligned} \tag{3.4}$$

with $\hat{a}$, $\hat{b}$ and $\hat{d}_f$ being respectively the estimated values of a, b and d_f. Since the longitudinal or the lateral forces and the estimated values of $\hat{a}$, $\hat{b}$ and $\hat{d}_f$ are always bounded in practical cases, we can use a positive constant D_1 in symbol of the upper bound of model error such that

$$|d_1(t)| \leq D_1. \tag{3.5}$$

Now, it is easy to obtain the following result.

Theorem 1: If the direct yaw-moment controller is constructed as

$$\begin{aligned} M_z = -[\hat{a}\left(F_{yfl} + F_{yfr}\right)\cos\delta + \frac{\hat{d}_f}{2}\left(F_{yfl} - F_{yfr}\right)\sin\delta \\ - \hat{b}\left(F_{yrl} + F_{yrr}\right) - I_z\dot{\omega}_{rd}] - K_1 I_z sign\,(s) \end{aligned} \tag{3.6}$$

with $K_1 > D_1$, the sliding variable s will finite-time converge to the origin.

Proof. Putting (3.6) into (3.3) yields

$$\begin{aligned} \dot{s} = \frac{1}{I_z}[(a-\hat{a})(F_{yfl} + F_{yfr})\cos\delta + (\frac{d_f}{2} - \frac{\hat{d}_f}{2})(F_{yfl} - F_{yfr})\sin\delta \\ - (b-\hat{b})(F_{yrl} + F_{yrr})] - K_1 sign(s). \end{aligned} \tag{3.7}$$

The Lyapunov function can be selected as

$$V_1(s) = \frac{1}{2}s^2. \tag{3.8}$$

Taking the derivative of (3.8) obtains

$$\begin{aligned} \dot{V}_1 &= s\dot{s} \\ &= -K_1|s| + \frac{1}{I_z}s[\tilde{a}(F_{yfl} + F_{yfr})\cos\delta + \frac{\tilde{d}_f}{2}(F_{yfl} - F_{yfr})\sin\delta - \tilde{b}(F_{yrl} + F_{yrr}] \\ &= -K_1|s| + d_1(t)s \\ &\le -(K_1 - D_1)|s| \end{aligned} \tag{3.9}$$

with $\tilde{a} = a - \hat{a}$, $\frac{\tilde{d}_f}{2} = \frac{d_f}{2} - \frac{\hat{d}_f}{2}$, $\tilde{b} = b - \hat{b}$.

Noting that $K_1 > D_1$, one has

$$\dot{V}_1 \le -cV_1^{1/2},$$

with $c = \sqrt{2}(K_1 - D_1)$. Based on the Lyapunov stability theory, the sliding variable s can converge to zero in finite time. We thus complete the proof of the theorem.

Remark 2: One can clearly see that the gain K_1 of controller (3.6) should be selected to guarantee $K_1 > D_1$. Nonetheless, the upper bound of disturbance D_1 is hard to be estimated accurately. Hence, we need a very large gain K_1 to suppress the disturbance, which may cause heavy chattering problems. Based on this, an AFOSM direct yaw-moment controller will be constructed later.

3.1.2. AFOSM controller design

Generally speaking, the system parameters in electric vehicle affecting the system performance seriously are hard to be detected. In this subsection, we are going to design the adaptive laws for electric vehicle system to estimate the parameter a, b and d_f based on the following rules

$$\dot{\hat{a}} = \frac{k_1}{I_z}s\left(F_{yfl} + F_{yfr}\right)\cos\delta \tag{3.10}$$

$$\frac{\dot{\hat{d}}_f}{2} = \frac{k_2}{I_z} s\left(F_{yfl} - F_{yfr}\right)\sin\delta \tag{3.11}$$

$$\dot{\hat{b}} = -\frac{k_3}{I_z} s\left(F_{yrl} + F_{yrr}\right) \tag{3.12}$$

where k_1, k_2, k_3 are all positive numbers. Now it is ready to present the following result.
Theorem 2: If the direct yaw-moment controller is constructed as

$$\begin{aligned} M_z = &-\hat{a}\left(F_{yfl} + F_{yfr}\right)\cos\delta + \hat{b}\left(F_{yfl} - F_{yfr}\right)\sin\delta \\ &- \frac{\hat{d}_f}{2}\left(F_{yrl} + F_{yrr}\right) + I_z\dot{\omega}_{rd} - K_2 I_z sign\,(s) \end{aligned} \tag{3.13}$$

with $K_2 > 0$, the sliding variable s can asymptotically converge to zero.
Proof. Redesign a Lyapunov function as

$$V_2 = \frac{1}{2}s^2 + \frac{1}{2k_1}\tilde{a}^2 + \frac{1}{2k_2}\left(\frac{\tilde{d}_f}{2}\right)^2 + \frac{1}{2k_3}\tilde{b}^2. \tag{3.14}$$

Taking derivative of (3.14), one has

$$\begin{aligned} \dot{V}_2 = &- K_2\,|s| + \frac{1}{I_z}s[\tilde{a}(F_{yfl}+F_{yfr})\cos\delta + \frac{\tilde{d}_f}{2}(F_{yfl}-F_{yfr})\sin\delta \\ &- \tilde{b}(F_{yrl}+F_{yrr})] + \frac{1}{k_1}\tilde{a}\dot{\tilde{a}} + \frac{1}{k_2}(\frac{\tilde{d}_f}{2})(\frac{\dot{\tilde{d}}_f}{2}) + \frac{1}{k_3}\tilde{b}\dot{\tilde{b}}. \end{aligned} \tag{3.15}$$

Since $\tilde{a} = a - \hat{a}$, $\frac{\tilde{d}_f}{2} = \frac{d_f}{2} - \frac{\hat{d}_f}{2}$, $\tilde{b} = b - \hat{b}$, it is derived from (3.15) that

$$\begin{aligned} \dot{V}_2 = &- K_2\,|s| + \frac{1}{I_z}s[\tilde{a}(F_{yfl}+F_{yfr})\cos\delta + \frac{\tilde{d}_f}{2}(F_{yfl}-F_{yfr})\sin\delta \\ &- \tilde{b}(F_{yrl}+F_{yrr})] - \frac{1}{k_1}\tilde{a}\dot{\hat{a}} - \frac{1}{k_2}(\frac{\tilde{d}_f}{2})(\frac{\dot{\hat{d}}_f}{2}) - \frac{1}{k_3}\tilde{b}\dot{\hat{b}}. \end{aligned} \tag{3.16}$$

By a simple calculation, one has

$$\begin{aligned} \dot{V}_2 = &- K_2\,|s| + [\frac{1}{I_z}s(F_{yfl} + F_{yfr})\cos\delta - \frac{1}{k_1}\dot{\hat{a}}]\tilde{a} + [\frac{1}{I_z}s(F_{yfl} \\ &- F_{yfr})\sin\delta - \frac{1}{k_2}\frac{\dot{\hat{d}}_f}{2}]\frac{\tilde{d}_f}{2} - [\frac{1}{I_z}s(F_{yrl} + F_{yrr}) + \frac{1}{k_3}\dot{\hat{b}}]\tilde{b}. \end{aligned} \tag{3.17}$$

It is noted that the adaptive laws (3.10), (3.11) and (3.12) are respectively generated by

$$\frac{1}{I_z}s\left(F_{yfl} + F_{yfr}\right)\cos\delta - \frac{1}{k_1}\dot{\hat{a}} = 0. \tag{3.18}$$

$$\frac{1}{I_z}s\left(F_{yfl} - F_{yfr}\right)\sin\delta - \frac{1}{k_2}\left(\frac{\dot{\hat{d}}_f}{2}\right) = 0. \tag{3.19}$$

$$\frac{1}{I_z} s \left(F_{yrl} + F_{yrr} \right) + \frac{1}{k_3} \dot{\hat{b}} = 0. \tag{3.20}$$

Substituting (3.10), (3.11) and (3.12) into (3.17), formula (3.15) can be rewritten as

$$\dot{V}_2 = -K_2 |s| \leq 0. \tag{3.21}$$

As long as the gain K_2 is positive, the sliding variable s can asymptotically converge to the origin.

Remark 3: Comparing the traditional FOSM direct yaw-moment controller (3.6) with the AFOSM controller (3.13), the adaptive laws used to estimate the parameters can indirectly reduce the disturbance. On this basis, we can conclude that the gain K_2 used to overcome the upper bound of the disturbance in (3.13) can be significantly reduced, which will greatly weaken the chattering. However, the high-frequency chattering problem in controller (3.13) still exists. In the next subsection, we will propose an ASTSM controller to further reduce the chattering.

Remark 4: It can be seen from Eqs (3.10)–(3.12) that k_1, k_2 and k_3 are the gains of the estimated values of a, d_f and b. Thus, one need first let k_1, k_2 and k_3 be large enough to ensure the estimated values are accurate. Additionally, these gains should be decreased until the distortion occurs.

3.1.3. ASTSM controller design

The STA was first presented in [42] by Arie Levant, which is a category of SOSM algorithm. Recently, the STA algorithm has been attracted much attention and widely applied to numerous plants, such as the permanent magnet synchronous motor [43, 44], the projective synchronisation of flexible manipulator [45], the liquid level regulation problem [46], aircraft system [47], electropneumatic actuator [48], etc.

The mathematical expression of STA is

$$\begin{cases} \dot{s} = -\alpha^* |s|^{1/2} \, sign\,(s) + v \\ \dot{v} = -\beta^* sign\,(s) \end{cases} \tag{3.22}$$

where s is sliding variable, α^* and β^* are gains, v is an intermediate variable.

System (3.3) can be rewritten as

$$\dot{s} = d_2\,(t) + bu \tag{3.23}$$

where $b = \frac{1}{I_z}$, $u = M_z$ and $d_2(t) = \frac{1}{I_z}[a(F_{yfl} + F_{yfr}) \cos\delta + \frac{d_f}{2}(F_{yfl} - F_{yfr}) \sin\delta - b(F_{yrl} + F_{yrr}) - I_z \dot{\omega}_{rd}]$ is regard as the unknown disturbance. As a matter of fact, ω_{rd} is a continuous funciton, which can also be seen from the simulation results. Therefore, one can reasonably assume that the disturbance $d_2(t)$ meets $\left|\dot{d}_2\,(t)\right| \leq D_2$ with $D_2 > 0$ being a constant.

By combining the traditional STA (3.22) with some adaptive laws, an adaptive super-twisting sliding-mode based DYC controller is constructed as follows

$$\begin{cases} M_z = \frac{1}{b}\left(-\hat{\alpha} |s|^{1/2} \, sign\,(s) + v\right) \\ \dot{v} = -\hat{\beta} sign\,(s) \end{cases} \tag{3.24}$$

$$\dot{\hat{\alpha}} = \rho_1 \left(\left(\lambda + 4\epsilon^2\right) |s|^{1/2} - 2\epsilon sign\,(s)\, v \right) \tag{3.25}$$

$$\dot{\hat{\beta}} = \rho_2 \left(-2\epsilon |s|^{1/2} + sign\,(s)\, v \right), \tag{3.26}$$

where λ, ϵ, ρ_1, ρ_2 are parameters. The adaptive laws (3.25) and (3.26) are used to update the controller gains in real time. On this basis,the following result will be obtained.

Theorem 3: If the direct yaw-moment controller is constructed as (3.24) with the adaptive laws (3.25) and (3.26), the sliding variable s can asymptotically converges to the origin.

Proof: By letting $x_1 = s$, $x_2 = v$, the closed-loop systems (3.23)–(3.26) can be written as

$$\dot{x}_1 = d_2(t) + bu \tag{3.27}$$

$$\begin{cases} M_z = \frac{1}{b}\left(-\hat{\alpha}\left|x_1\right|^{1/2} sign\left(x_1\right) + x_2\right) \\ \dot{x}_2 = -\hat{\beta} sign\left(x_1\right) \end{cases} \tag{3.28}$$

$$\dot{\hat{\alpha}} = \rho_1\left(\left(\lambda + 4\epsilon^2\right)\left|x_1\right|^{1/2} - 2\epsilon sign\left(x_1\right) x_2\right) \tag{3.29}$$

$$\dot{\hat{\beta}} = \rho_2\left(-2\epsilon\left|x_1\right|^{1/2} + sign\left(x_1\right) x_2\right) \tag{3.30}$$

A new state vector is introduced as follows:

$$\xi = \begin{pmatrix} \left|x_1\right|^{1/2} sign\left(x_1\right) & x_2 \end{pmatrix}^T. \tag{3.31}$$

Taking the derivative of (3.31) and combining the system (3.27), one has

$$\begin{aligned} \dot{\xi} &= \begin{pmatrix} \frac{1}{2\left|x_1\right|^{1/2}}\left(-\hat{\alpha}\left|x_1\right|^{1/2} sign\left(x_1\right) + x_2\right) \\ -\hat{\beta} sign\left(x_1\right) + \dot{d}_2(t) \end{pmatrix} \\ &= \frac{1}{\left|x_1\right|^{1/2}}\left(\hat{A}\xi + Bh\right) \end{aligned} \tag{3.32}$$

which can be written as

$$\dot{\xi}^T = \frac{1}{\left|x_1\right|^{1/2}}\left(\xi^T \hat{A}^T + B^T h\right) \tag{3.33}$$

where $A = \begin{pmatrix} -\frac{\alpha}{2} & \frac{1}{2} \\ -\beta & 0 \end{pmatrix}$, $\hat{A} = \begin{pmatrix} -\frac{\hat{\alpha}}{2} & \frac{1}{2} \\ -\hat{\beta} & 0 \end{pmatrix}$, $\tilde{A} = A - \hat{A} = \begin{pmatrix} -\frac{\tilde{\alpha}}{2} & 0 \\ -\tilde{\beta} & 0 \end{pmatrix}$, $B = \begin{pmatrix} 0 & 1 \end{pmatrix}^T$, $h = \dot{d}_2(t)\left|x_1\right|^{1/2}$, α, β are respectively the upper bound of adaptive laws $\hat{\alpha}$ and $\hat{\beta}$, which guarantees that $\tilde{\alpha}$ and $\tilde{\beta}$ are greater than 0.

A Lyapunov function is defined as follows

$$V_0 = \xi^T P \xi \tag{3.34}$$

where $P = \begin{pmatrix} \lambda + 4\varepsilon^2 & -2\varepsilon \\ -2\varepsilon & 1 \end{pmatrix}$ is a positive definite matrix.

From (3.34), one has

$$\begin{aligned}\dot{V}_0 &= \dot{\xi}^T P\xi + \xi^T P\dot{\xi} \\ &= \frac{1}{|x_1|^{1/2}}\left(\xi^T \hat{A}^T + B^T h\right) P\xi + \xi^T P \frac{1}{|x_1|^{1/2}}\left(\hat{A}\xi + Bh\right) \\ &= \frac{1}{|x_1|^{1/2}}\xi^T\left(\hat{A}^T P + P\hat{A}\right)\xi + \frac{1}{|x_1|^{1/2}}\left(B^T P\xi + \xi^T PB\right)h \\ &= \frac{1}{|x_1|^{1/2}}\xi^T\left(A^T P + PA\right)\xi - \frac{1}{|x_1|^{1/2}}\xi^T\left(\tilde{A}^T P + P\tilde{A}\right)\xi \\ &\quad + \frac{1}{|x_1|^{1/2}}\left(B^T P\xi + \xi^T PB\right)h\end{aligned} \tag{3.35}$$

Note that

$$\frac{1}{|x_1|^{1/2}}\xi^T(\tilde{A}^T P + P\tilde{A})\xi = -\tilde{\alpha}((\lambda + 4\epsilon^2)|x_1|^{1/2} - 2\epsilon sign(x_1)x_2) - 2\tilde{\beta}(-2\epsilon|x_1|^{1/2} + sign(x_1)x_2) \tag{3.36}$$

and

$$\begin{aligned}\Gamma &= \frac{1}{|x_1|^{1/2}}\xi^T\left(A^T P + PA\right)\xi + \frac{1}{|x_1|^{1/2}}\left(B^T P\xi + \xi^T PB\right)h \\ &= \frac{1}{|x_1|^{1/2}}\xi^T\left(A^T P + PA\right)\xi + \frac{1}{|x_1|^{1/2}}2\xi^T PBh\end{aligned} \tag{3.37}$$

Applying Young's inequality to (3.37) yields

$$\begin{aligned}\Gamma &\le \frac{1}{|x_1|^{1/2}}\left(\xi^T\left(A^T P + PA + PBB^T P\right)\xi + h^2\right) \\ &= \frac{1}{|x_1|^{1/2}}\left(\xi^T\left(A^T P + PA + PBB^T P\right)\xi + \left(\dot{d}_2(t)\right)^2|x_1|\right)\end{aligned} \tag{3.38}$$

Namely

$$\begin{aligned}\Gamma &\le \frac{1}{|x_1|^{1/2}}\left(\xi^T\left(A^T P + PA + PBB^T P\right)\xi + D_2^2\xi^T C^T C\xi\right) \\ &= \frac{1}{|x_1|^{1/2}}\xi^T\left(A^T P + PA + PBB^T P + D_2^2 C^T C\right)\xi\end{aligned} \tag{3.39}$$

with $C = \begin{pmatrix}1 & 0\end{pmatrix}$.
Letting $Q = -\left(A^T P + PA + PBB^T P + D_2^2 C^T C\right)$, one has

$$Q = \begin{pmatrix}Q_{11} & Q_{12} \\ Q_{21} & Q_{22}\end{pmatrix} \tag{3.40}$$

with
$Q_{11} = \alpha\left(\lambda + 4\varepsilon^2\right) - 4\beta\varepsilon - 4\varepsilon^2 - D_2^2$
$Q_{12} = Q_{21} = -\frac{1}{2}\left(\lambda + 4\varepsilon^2\right) - \alpha\varepsilon + \beta + 2\varepsilon$
$Q_{22} = 2\varepsilon - 1.$

To ensure the positive definiteness of matrix Q, we enforce $Q_{11} > 0$ and $Q_{11}Q_{22} - Q_{12}Q_{21} > 0$.

The matrix Q can be positive definite if

$$\begin{cases} \alpha = \frac{-\frac{1}{2}\left(\lambda+4\varepsilon^2\right)+\beta+2\varepsilon}{\varepsilon} \\ \varepsilon > \frac{1}{2} \\ \lambda > \max\left\{\frac{4\beta\varepsilon+4\varepsilon^2+D_2^2}{\alpha} - 4\varepsilon^2, 0\right\}. \end{cases} \tag{3.41}$$

Inequality (3.39) can be simplified as

$$\Gamma = -\frac{1}{|x_1|^{1/2}}\xi^T Q\xi \leq -\lambda_{\min}(Q)\|\xi\|_2 \leq 0. \tag{3.42}$$

Equation (3.35) is rewritten as

$$\begin{aligned} \dot{V}_0 \leq \tilde{\alpha}\left(\left(\lambda + 4\epsilon^2\right)|x_1|^{1/2} - 2\epsilon sign(x_1)\, x_2\right) \\ + 2\tilde{\beta}\left(-2\epsilon|x_1|^{1/2} + sign(x_1)\, x_2\right). \end{aligned} \tag{3.43}$$

Construct the whole Lyapunov function as

$$V = V_0 + \frac{1}{2\rho_1}\tilde{\alpha}^2 + \frac{1}{2\rho_2}\tilde{\beta}^2. \tag{3.44}$$

The derivative of Eq (3.44) is given as follows

$$\begin{aligned} \dot{V} \leq \tilde{\alpha}\left(\left(\lambda + 4\epsilon^2\right)|x_1|^{1/2} - 2\epsilon sign(x_1)\, x_2\right) \\ + 2\tilde{\beta}\left(-2\epsilon|x_1|^{1/2} + sign(x_1)\, x_2\right) - \frac{1}{\rho_1}\tilde{\alpha}\dot{\tilde{\alpha}} - \frac{1}{\rho_2}\tilde{\beta}\dot{\tilde{\beta}}. \end{aligned} \tag{3.45}$$

We further have

$$\begin{aligned} \dot{V} \leq & \tilde{\alpha}\left(\left(\lambda + 4\epsilon^2\right)|x_1|^{1/2} - 2\epsilon sign(x_1)x_2 - \frac{1}{\rho_1}\dot{\tilde{\alpha}}\right) \\ & + 2\tilde{\beta}\left(-2\epsilon|x_1|^{1/2} + sign(x_1)x_2 - \frac{1}{\rho_2}\dot{\tilde{\beta}}\right). \end{aligned} \tag{3.46}$$

Substituting (3.29), (3.30) into (3.46), inequality (3.46) can be simplified as

$$\dot{V} \leq 0. \tag{3.47}$$

This implies that the state x_1 can asymptotically converges to the origin. Thus, the proof is finished.

3.2. Lower controller

Additional yaw moment is used to act on each wheel by changing the drive torque of the inner and outer wheels. The relationship between the longitudinal force of tire and the torque of motor is

$$F_{xij} = \frac{T_{ij}}{R}, \tag{3.48}$$

where F_{xij} is the longitudinal force, T_{ij} is the braking or driving torques of wheels and R is the tire radius.

The braking or driving torque acting on each wheel can be obtained as follows [49]

$$\begin{aligned} T_{fl} &= \frac{F_{zfl}}{F_z}\frac{M_z}{\left(-d_f/2\right)\cos\delta + \text{asin}\delta}R \\ T_{fr} &= \frac{F_{zfr}}{F_z}\frac{M_z}{\left(d_f/2\right)\cos\delta + \text{asin}\delta}R \\ T_{rl} &= -\frac{F_{zrl}}{F_z}\frac{M_z}{2d_r}R \\ T_{rr} &= \frac{F_{zrr}}{F_z}\frac{M_z}{2d_r}R \end{aligned} \tag{3.49}$$

with F_{zij} being the vertical load.

Finally, considering the constraints such as motor output and road adhesion coefficient, the torque constraints calculated by formula (3.49) are as follows

$$\left|T_{ij}\right| \leq min\left(\mu R F_{zij}, T_{max}\right). \tag{3.50}$$

Remark 5: The advantages of ASTSM can be summarized as follows. On the one hand, by combining adaptive control technique and STA, the proposed ASTSM in this paper can avoid the issue of excessive fixed gain estimation, which further weakens the chattering. On the other hand, as compared to the existing ASTSM, the adaptive law in the proposed ASTSM is not required to adopt the form of piecewise function, which reduces the complexity of the parameter adjustment process. However, it also should be pointed out that by comparing with the conventional super-twisting algorithm, the ASTSM is more complex in general since more adjustable parameters are added. Moreover, some extra assumptions on the disturbance are required.

Remark 6: Several possible applications of the proposed DYC system are listed as follows. One possible application is in autonomous vehicles, where the DYC system can be used to improve the vehicle's stability and handling during high-speed maneuvers, emergency avoidance or adverse weather conditions. Another possible application is in electric vehicles, where the DYC system can be integrated with regenerative braking to improve the vehicle's energy efficiency and reduce brake wear.

In addition to these applications, there are several possible extensions of the proposed DYC system that can improve its performance or make it more adaptable to different situations. One extension is the use of machine learning techniques, such as neural networks or reinforcement learning, to learn the optimal control parameters for the DYC system in different driving scenarios. Another extension is the use of multiple actuators to generate the yaw moment, which can provide the greater flexibility and control over the vehicle's behavior.

4. Simulation

In order to compare the direct yaw-moment controllers (3.6), (3.13) and (3.24), we use cosimulation environment including *Carsim* (C-Class Hatchback) and Simulink to conduct simulations for driving conditions under side-wind disturbances. In the process of simulation test, only the interference of

side wind is considered, while the external influence such as the environment with uneven ground and disturbed by external forces is not considered. The simulation test parameters are selected according to Carsim software in Table 1.

Table 1. Electric vehicle model parameters.

Symbol	Value	Unit
m	1412	kg
a	1.015	m
b	1.895	m
I_z	1536.7	$kg \cdot m^2$
K_1	−176142	N/rad
K_2	−139046	N/rad
d_f	1.65	m
d_r	1.65	m

4.1. Double lane change

To demonstrate the availability of the proposed direct yaw-moment controllers, a double lane change condition under lateral wind is designed for simulations. The parameters of direct yaw-moment controllers (3.6), (3.13) and (3.24) are shown in Table 2. The simulated car model is driven at a high speed 80 km/h. Meanwhile, the road adhesion coefficient μ is 0.5. Figures 3–7 show the simulation results. The side wind as an external disturbance is depicted in Figure 3, and its maximum value can reach 800 (N.m), which can better prove the effectiveness of the presented solution.

Table 2. Controllers' parameters under double lane change condition.

Controller	Parameters
FOSM controller (3.6)	$K_1 = 2$
AFOSM controller (3.13)	$k_1 = k_2 = k_3 = 3000$, $K_2 = 0.35$
ASTSM controller (3.24)	$\rho_1 = 0.5$, $\rho_2 = 0.5$ $\lambda = 200$, $\varepsilon = 5$

In Figure 4, all controllers (3.6), (3.13) and (3.24) designed in this work can make the actual yaw rate track its expected values. From Figure 5, as comparison with no control, the sideslip angle is in a suitable range. The sideslip angle is not taken as the controlled quantity, and hence it does not fully track the given value, which does not influence the improvement of the performance of the electric vehicle. In Figures 4–6, the performance of system without control is worse than the system using other three controllers, which also exhibits the good performance of the sliding mode controllers (3.6), (3.13) and (3.24). One can clearly see from Figure 7, due to the fact that the gain K_2 in AFOSM controller (3.13) is smaller than the gain K_1 in FOSM controller (3.6), AFOSM controller (3.13) has the less chattering. Meanwhile, AFOSM controller (3.13) still has heavy chattering since it includes discontinuous sign functions. In contrast, ASTSM controller (3.24) has significantly weakened the problem of chattering by putting the discontinuous terms into the derivative of the sliding variable, which reflects the effectiveness and superiority of the proposed solution. To sum up, the proposed

SMC strategy ensures the vehicle driving stability and improves the disturbance rejection performance of the vehicle.

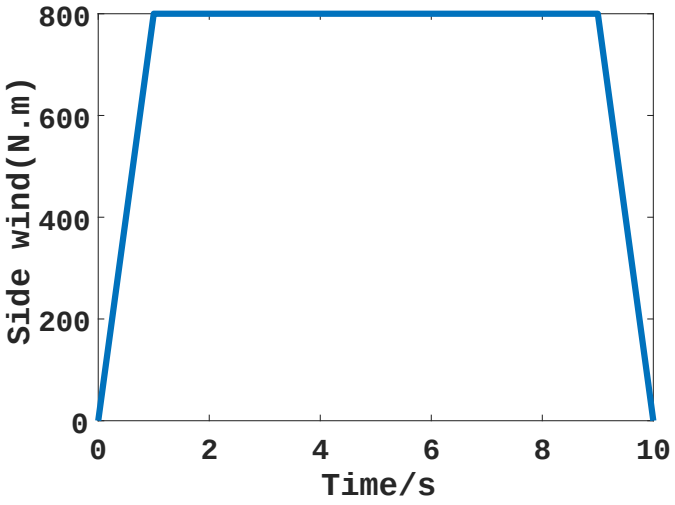

Figure 3. Side wind.

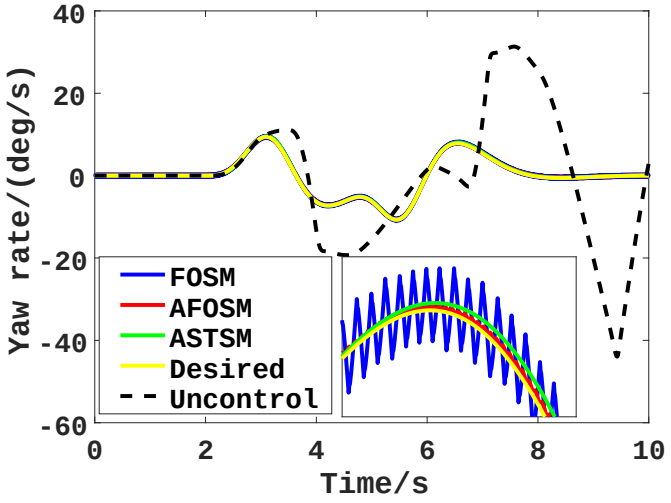

Figure 4. Yaw rate under double lane change.

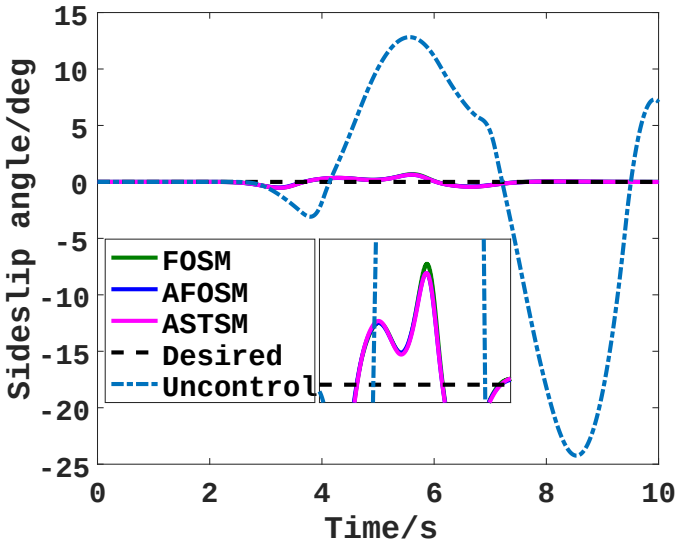

Figure 5. Sideslip angle under double lane change.

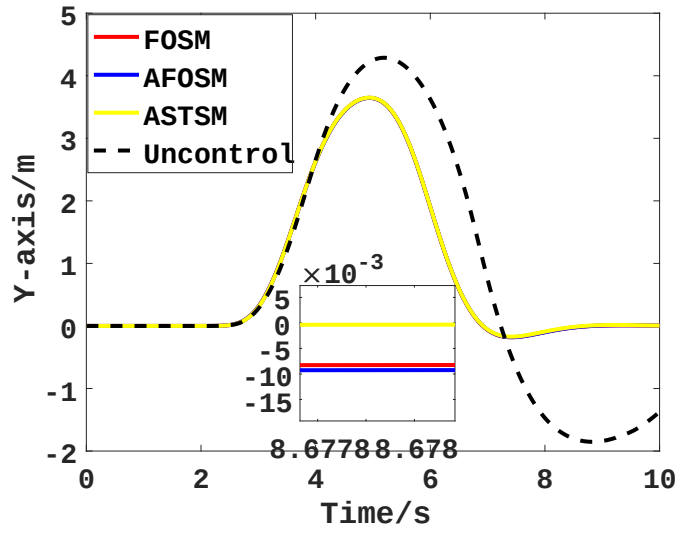

Figure 6. Lateral position under double lane change.

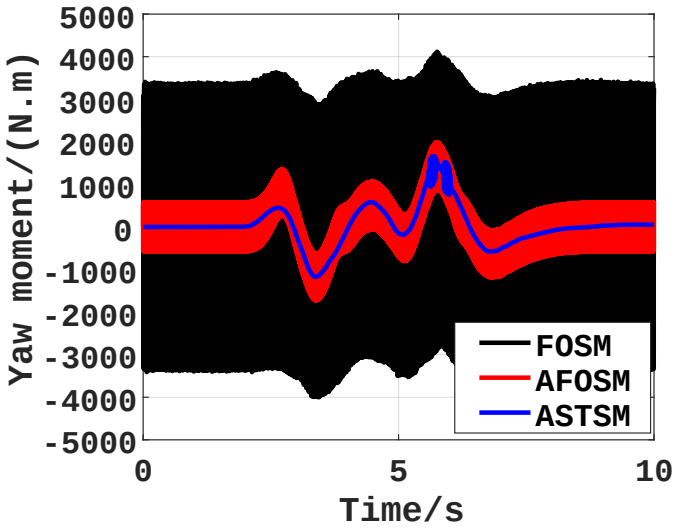

Figure 7. Yaw moment under double lane change.

4.2. Snake lane

Table 3. Controllers' parameters under snake lane condition.

Controller	Parameters
FOSM controller (3.6)	$K_1 = 2$
AFOSM controller (3.13)	$k_1 = k_2 = k_3 = 3000$, $K_2 = 0.35$
ASTSM controller (3.24)	$\rho_1 = 0.2, \rho_2 = 0.1, \lambda = 20, \varepsilon = 5$

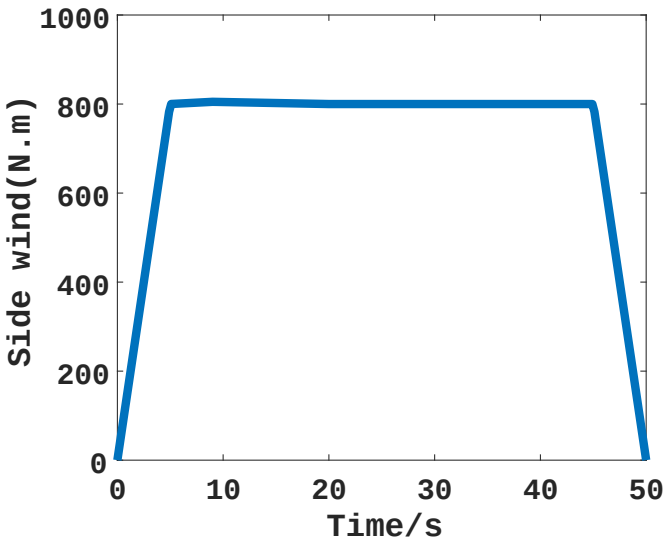

Figure 8. Side wind under snake lane condition.

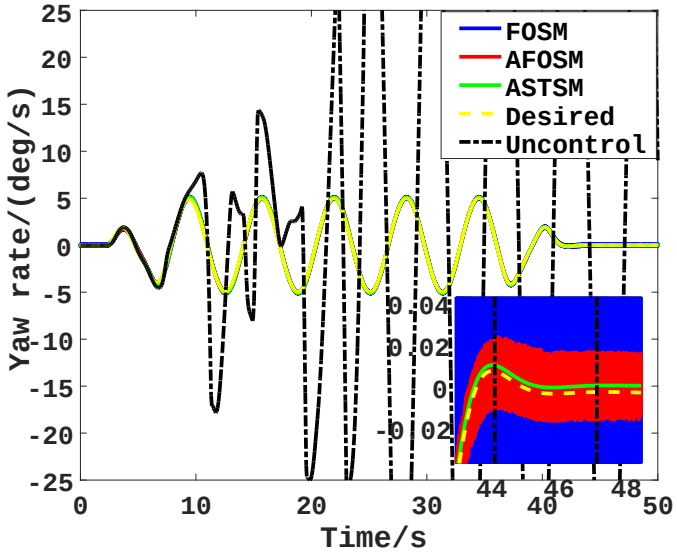

Figure 9. Yaw rate under snake lane condition.

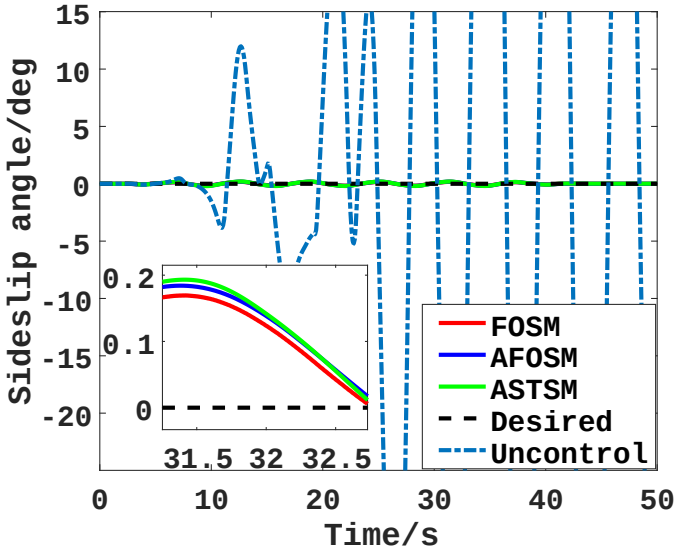

Figure 10. Sideslip angle under snake lane condition.

The snake lane condition differs from the double lane change condition, which is more complex. It is also utilized to test the effectiveness of the proposed controllers. There are more than ten sharp turns in this condition, which is a bigger challenge for the sliding mode controllers (3.6), (3.13) and (3.24). The simulation time of the whole experiment is up to 50 seconds, while only 10 seconds in the double lane change condition. The parameters of direct yaw-moment controllers (3.6), (3.13) and (3.24) in snake lane condition are shown in Table 3. Simulation results can be seen in Figures 8–12. In Figure 8, the maximum value of the side wind is also set as 800 (N.m). In Figures 9 and 10, without the use of sliding mode controllers, the stability index will be out of control so that the electric vehicle will lose stability. In Figure 11, by comparing with the situation without control, all the sliding mode controllers (3.6), (3.13) and (3.24) can make the electric vehicle keep a good trajectory. In Figure 12, ASTSM control method (3.24) is much better than FOSM control method (3.6) and AFOSM control method

(3.13). Owing to the discontinuous term of FOSM controller, FOSM controller (3.6) and AFOSM controller (3.13) have the heavy chattering, while the chattering in ASTSM controller (3.24) has been significantly reduced. All simulation results show that the SMC improves the system performance.

By the way, it should be mentioned that improved SMC algorithms proposed in the paper can avoid the excessive chattering caused by fixed gain. However, they depend on the selection of adaptive parameters. If the parameter selection is not appropriate, it may cause some problems such as parameter drift. Therefore, the parameters need to be restricted in practical engineering applications.

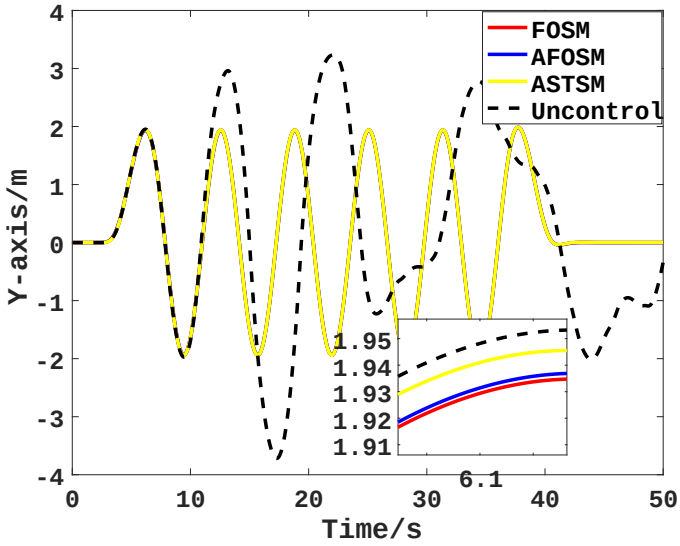

Figure 11. Lateral position under snake lane condition.

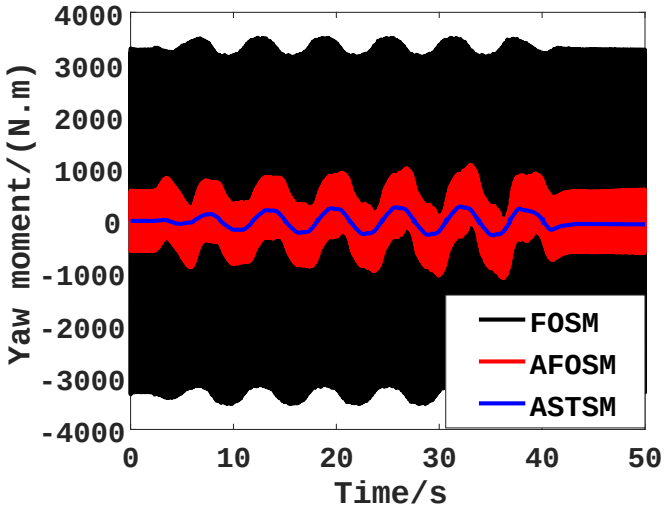

Figure 12. Yaw moment under snake lane condition.

5. Conclusions

In this paper, the proposed ASMC and ASTSMC for DYC systems have been proved remarkable in tracking desired electric vehicle behaviors. Although the AFOSM controller attenuates the chattering by utilizing the adaptive laws, the chattering still exists attributed to discontinuous sign functions. To address this issue, an ASTSM control method puts the discontinuous sign functions into the derivative of the sliding variable, which fundamentally reduces the chattering. Finally, it can be seen by simulation results that the proposed ASTSM controller is more effective in improving the driving stability.

Acknowledgments

This research was supported by the National Natural Science Foundation of China under Grant 61973142 and Grant 62203188, the Jiangsu Natural Science Foundation for Distinguished Young Scholars under Grant BK20180045, the Natural Science Foundation of Jiangsu Province under Grant BK20220517, the China Postdoctoral Science Foundation under Grant 2022M721386 and the Priority Academic Program Development of Jiangsu Higher Education Institutions.

Conflict of interest

The authors declare there is no conflict of interest.

References

1. L. Ma, K. Mei, S. Ding, T. Pan, Design of adaptive fuzzy fixed-time HOSM controller subject to asymmetric output constraints, *IEEE Trans. Fuzzy Syst.*, **2023** (2023). https://doi.org/10.1109/TFUZZ.2023.3241147
2. Y. Tang, X. Wu, P. Shi, F. Qian, Input-to-state stability for nonlinear systems with stochastic impulses, *Automatica*, **113** (2020), 108766. https://doi.org/10.1016/j.automatica.2019.108766
3. B. Xu, Q. Jiang, W. Ji, S. Ding, An improved three-vector-based model predictive current control method for surface-mounted PMSM drives, *IEEE Trans. Transp. Electrif.*, **8** (2022), 4418–4430. https://doi.org/10.1109/TTE.2022.3169515
4. Q. K. Hou, S. H. Ding, X. H. Yu, Composite super-twisting sliding mode control design for PMSM speed regulation problem based on a novel disturbance observer, *IEEE Trans. Energy Convers.*, **36** (2021), 2591–2599. https://doi.org/10.1109/tec.2020.2985054
5. Y. Wu, L. F. Wang, J. Z. Zhang, F. Li, Robust vehicle yaw stability controlby active front steering with active disturbance rejection controller, in *Proceedings of the Institution of Mechanical Engineers Part I Journal of Systems and Control Engineering*, (2018). https://doi.org/10.1177/0959651818813515
6. J. Zhang, H. Wang, M. Ma, M. Yu, A. Yazdani, Active front steering-based electronic stability control for steer-by-wire vehicles via terminal sliding mode and extreme learning machine, *IEEE Trans. Veh. Technol.*, **69** (2020), 14713–14726. https://doi.org/10.1109/TVT.2020.3036400

7. Y. C. Zhu, L. Ma, Composite chattering-free discrete-time sliding mode controller design for active front steering system of electric vehicles, *Nonlinear Dyn.*, **105** (2021), 301–313. https://doi.org/10.1007/s11071-021-06465-5
8. A. Aksjonov, K. Augsburg, V. Vodovozov, Design and Simulation of the Robust ABS and ESP Fuzzy Logic Controller on the Complex Braking Maneuvers, *Appl. Sci.*, **6** (2016). https://doi.org/10.3390/app6120382
9. J. H. Guo, Y. G. Luo, C. Hu, C. Tao, K. Q. Li, Robust combined lane keeping and direct yaw moment control for intelligent electric vehicles with time delay, *Int. J. Autom. Technol.*, **20** (2019), 289–296. https://doi.org/10.1007/s12239-019-0028-5
10. S. H. Ding, J. L. Sun, Direct yaw-moment control for 4WID electric vehicle via finite-time control technique, *Nonlinear Dyn.*, **88** (2016), 239–254. https://doi.org/10.1007/s11071-016-3240-0
11. B. Xu, X. Cui, W. Ji, H. Yuan, J. Wang, Apple grading method design and implementation for automatic grader based on improved YOLOv5, *Agriculture*, **13** (2023), 124. https://doi.org/10.3390/agriculture13010124
12. B. Xu, L. Zhang, W. Ji, Improved non-singular fast terminal sliding mode control with disturbance observer for PMSM drives, *IEEE Trans. Transp. Electrification*, **7** (2021), 2753–2762. https://doi.org/10.1109/TTE.2021.3083925
13. J. Sun, J. Yi, Z. Pu, Fixed-time adaptive fuzzy control for uncertain nonstrict-feedback systems with time-varying constraints and input saturations, *IEEE Trans. Fuzzy Syst.*, **30** (2022), 1114–1128. https://doi.org/10.1109/TFUZZ.2021.3052610
14. X. Li, D. W. C. Ho, J. Cao, Finite-time stability and settling-time estimation of nonlinear impulsive systems, *Automatica*, **99** (2019), 361–368. https://doi.org/10.1016/j.automatica.2018.10.024
15. K. Mei, C. Qian, S. Ding, Design of adaptive SOSM controller subject to disturbances with unknown magnitudes, *IEEE Trans. Circuits Syst. I*, **70** (2023), 2133–2142. https://doi.org/10.1109/TCSI.2023.3241291
16. K. Mei, S. Ding, X. Yu, A generalized supertwisting algorithm, *IEEE Trans. Cybern.*, **2022** (2022). https://doi.org/10.1109/TCYB.2022.3188877
17. S. Ding, B. Zhang, K. Mei, J. Park, Adaptive fuzzy SOSM controller design with output constraints, *IEEE Trans. Fuzzy Syst.*, **30** (2022), 2300–2311. https://doi.org/10.1109/TFUZZ.2021.3079506.
18. X. Li, X. Yang, S. Song, Lyapunov conditions for finite-time stability of time-varying time-delay systems, *Automatica*, **103** (2019), 135–140. https://doi.org/10.1016/j.automatica.2019.01.031
19. X. Li, X. Yan, J. Cao, Event-triggered impulsive control for nonlinear delay systems, *Automatica*, **117** (2020), 108981. https://doi.org/10.1016/j.automatica.2020.108981
20. J. H. Guo, J. Y. Wang, Y. G. Luo, K. Q. Li, Takagi–Sugeno fuzzy-based robust H_∞ integrated lane-keeping and direct yaw moment controller of unmanned electric vehicles, *IEEE/ASME Trans. Mech.*, **26** (2020), 2151–2162. https://doi.org/10.1109/TMECH.2020.3032998
21. K. Mei, S. Ding, W. X. Zheng, Fuzzy adaptive SOSM based control of a type of nonlinear systems, *IEEE Trans. Circuits Syst. II*, **69** (2022), 1342–1346. https://doi.org/10.1109/TCSII.2021.3116812

22. X. K. He, K. M. Yang, Y. L. Liu, X. W. Ji, A novel direct yaw moment control system for autonomous vehicle, *SAE Tech. Paper*, **2018** (2018). https://doi.org/10.4271/2018-01-1594
23. S. Ding, Q. Hou, H. Wang, Disturbance-observer-based second-order sliding mode controller for speed control of PMSM drives, *IEEE Trans. Energy Convers.*, **38** (2023),100–110. https://doi.org/10.1109/TEC.2022.3188630
24. L. Hind, D. Moustapha, T. Reine, C. Ali, Yaw moment Lyapunov based control for in-wheel-motor-drive electric vehicle, *IFAC-PapersOnLine*, **50** (2017), 13828–13833. https://doi.org/10.1016/j.ifacol.2017.08.2189
25. J. Song, W. X. Zheng, Y. G. Niu, Self-triggered sliding mode control for networked PMSM speed regulation system: A PSO-optimized super-twisting algorithm, *IEEE Trans. Ind. Electron.*, **69** (2021), 763–773. https://doi.org/10.1109/TIE.2021.3050348
26. S. H. Ding, B. B. Zhang, K. Q. Mei, J. H. Park, Adaptive fuzzy SOSM controller design with output constraints, *IEEE Trans. Fuzzy Syst.*, **30** (2021), 2300–2311. https://doi.org/10.1109/TFUZZ.2021.3079506
27. S. H. Ding, K. Q. Mei, X. H. Yu, Adaptive second-order sliding mode control: A Lyapunov approach, *IEEE Trans. Autom. Control*, **67** (2021), 5392–5399. https://doi.org/10.1109/TAC.2021.3115447
28. S. H. Ding, L. Liu, W. X. Zheng, Sliding mode direct yaw-moment control design for in-wheel electric vehicles, *IEEE Trans. Ind. Electron.*, **64** (2017), 6752–6762. https://doi.org/10.1109/tie.2017.2682024
29. B. Lenzo, M. Zanchetta, A. Sorniotti, P. Gruber, W. D. Nijs, Yaw rate and sideslip angle control through single input single output direct yaw moment control, *IEEE Trans. Control Syst. Technol.*, **29** (2021), 124–139. https://doi.org/10.1109/TCST.2019.2949539
30. C. Y. Fu, H. Reza, K. N. Li, M. H. Hu, A novel adaptive sliding mode control approach for electric vehicle direct yaw-moment control, *Adv. Mech. Eng.*, **10** (2018), 1–12. https://doi.org/10.1177/1687814018803179
31. W. Qi, H. Su, A Cybertwin based multimodal network for ECG patterns monitoring using deep learning, *IEEE Trans. Ind. Inf.*, **18** (2022), 6663–6670. https://doi.org/10.1109/TII.2022.3159583
32. Y. Shi, L. Li, J. Yang, Y. Wang, S. Hao, Center-based transfer feature learning with classifier adaptation for surface defect recognition, *Mech. Syst. Signal Process.*, **188** (2023), 110001. https://doi.org/10.1016/j.ymssp.2022.110001
33. S. Roy, S. Baldi, L. M. Fridman, On adaptive sliding mode control without a priori bounded uncertainty, *Automatica*, **111** (2020), 108650. https://doi.org/10.1016/j.automatica.2019.108650
34. Z. Lv, Y. Wu, X. Sun, Q. Wang, Fixed-time control for a quadrotor with a cable-suspended load, *IEEE Trans. Intell. Trans. Syst.*, **23** (2022), 21932–21943. https://doi.org/10.1109/TITS.2022.3180733
35. Q. Hou, S. Ding, GPIO based super-twisting sliding mode control for PMSM, *IEEE Trans. Circuits Syst. II*, **68** (2021), 747–751. https://doi.org/10.1109/TCSII.2020.3008188
36. Z. Lv, Q. Zhao, S. Li, Y. Wu, Finite-time control design for a quadrotor transporting a slung load, *Control Eng. Prac.*, **122** (2022), 105082. https://doi.org/10.1016/j.conengprac.2022.105082

37. Y. Tang, X. Jin, Y. Shi, W. Du, Event-triggered attitude synchronization of multiple rigid body systems with velocity-free measurements, *Automatica*, **143** (2022), 110460. https://doi.org/10.1016/j.automatica.2022.110460
38. Y. Tang, D. Zhang, P. Shi, W. Zhang, F. Qian, Event-based formation control for nonlinear multiagent systems under DoS attacks, *IEEE Trans. Autom. Control*, **66** (2021), 452–459. https://doi.org/10.1109/TAC.2020.2979936
39. W. W. Chen, X. T. Liang, Q. D. Wang, L. F. Zhao, X. Wang, Extension coordinated control of four wheel independent drive electric vehicles by AFS and DYC, *Control Eng. Prac.*, **101** (2020), 1242–1258. https://doi.org/10.1016/j.conengprac.2020.104504
40. S. B. Zheng, H. J. Tang, J. Hou, Z. Z. Han, Y. Zhang, Controller design for vehicle stability enhancement, *Control Eng. Prac.*, **14** (2006), 1413–1421. https://doi.org/10.1016/j.conengprac.2005.10.005
41. R. Rajesh, *Vehicle Dynamics and Control*, Springer Science & Business Media, 2011.
42. L. Arie, Sliding order and sliding accuracy in sliding mode control, *Int. J. Control*, **58** (1993), 1247–1263. https://doi.org/10.1080/00207179308923053
43. D. L. Liang, J. Li, R. H. Qu, W. B. Kong, Adaptive second-order sliding-mode observer for PMSM sensorless control considering VSI nonlinearity, *IEEE Trans. Power Electron.*, **33** (2017), 8994–9004. https://doi.org/10.1109/TPEL.2017.2783920
44. Q. K Hou, S. H. Ding, X. H. Yu, K. Q. Mei, A super-twisting-like fractional controller for SPMSM drive system, *IEEE Trans. Ind. Electron.*, **69** (2021), 9376–9384. https://doi.org/10.1109/TIE.2021.3116585
45. K. Q. Mei, S. H. Ding, C. C. Chen, Fixed-time stabilization for a class of output-constrained nonlinear systems, *IEEE Trans. Syst. Man Cybern. Syst.*, **52** (2022), 6498– 6510. https://doi.org/10.1109/tsmc.2022.3146011
46. G. Gandikota, D. K. Das, Terminal sliding mode disturbance observer based adaptive super twisting sliding mode controller design for a class of nonlinear system, *Eur. J. Control*, **57** (2021), 232–241. https://doi.org/10.1016/j.ejcon.2020.05.004
47. B. B. Yan, P. Dai, R. F. Liu, M. Z. Xing, S. X. Liu, Adaptive super-twisting sliding mode control of variable sweep morphing aircraft, *Aerosp. Sci. Technol.*, **92** (2019), 198–210. https://doi.org/10.1016/j.ast.2019.05.063
48. S. Yuri, T. Mohammed, P. Franck, A novel adaptive-gain supertwisting sliding mode controller: Methodology and application, *Automatica*, **48** (2012), 759–769. https://doi.org/10.1016/j.automatica.2012.02.024
49. L. Zhai, T. M. Sun, J. Wang, Electronic stability control based on motor driving and braking torque distribution for a four in-wheel motor drive electric vehicle, *IEEE Trans. Veh. Technol.*, **65** (2016), 4726–4739. https://doi.org/10.1109/TVT.2016.2526663

AIMS Press